ORNL/TM-2024/3273

Comparison of Temperature-Dependent Cross Section Treatments Within the Shift Monte Carlo Radiation Transport Code

Amanda M. Bachmann
Seth R. Johnson
Elliott D. Biondo
Shane W. D. Hart
Thomas M. Evans

January 31, 2024

OAK RIDGE National Laboratory

ORNL IS MANAGED BY UT-BATTELLE LLC FOR THE US DEPARTMENT OF ENERGY

Front cover

ORNL/TM-2024/3273

Computational Sciences and Engineering Division

COMPARISON OF TEMPERATURE-DEPENDENT CROSS SECTION TREATMENTS WITHIN THE SHIFT MONTE CARLO RADIATION TRANSPORT CODE

Amanda M. Bachmann
Seth R. Johnson
Elliott D. Biondo
Shane W. D. Hart
Thomas M. Evans

January 31, 2024

Prepared by
OAK RIDGE NATIONAL LABORATORY
Oak Ridge, TN 37831
managed by
UT-BATTELLE LLC
for the
US DEPARTMENT OF ENERGY
under contract DE-AC05-00OR22725

CONTENTS

LIST OF FIGURES

LIST OF TABLES

ABSTRACT

Multiple calculation methods have been developed to account for Doppler broadening of cross sections in Monte Carlo radiation transport simulations. This work compares the accuracy and performance of four different broadening methods, including an on-the-fly multipole treatment, applied to three different geometries of increasing complexity, including a nuclear reactor assembly with a realistic temperature profile. The comparisons reveal how the combination of physics implementations in the Shift Monte Carlo code result in slightly different temperature-dependent behavior, and different levels of performance, for a variety of materials and situations.

1. INTRODUCTION

Accurate cross section data is paramount for accurate Monte Carlo (MC) radiation transport. This is especially true of multiphysics calculations, in which neutronics is coupled with thermal hydraulics. Changes in cross section data from temperature changes affect radiation transport calculations, which affect thermal hydraulics calculations. To accurately capture the effects of Doppler broadening on cross section data, multiple mathematical models and computational methods have been established, each with its own advantages and disadvantages.

The traditional method of accounting for temperature-dependent effects is to process cross section data at 0 K using codes such as AMPX Dunn and Greene, n.d. or NJOY Macfarlane 2000 to obtain cross section values of a given nuclide for a grid of temperatures. The 0 K and processed cross section data are stored in a data library for use during a radiation transport simulation. When a material temperature is specified in the problem, the cross section data at the nearest temperature grid point are used. Although it is a simple way of accounting for temperature-dependent effects, this method is limited by the number of temperature grid points with stored cross section data. The more grid points with stored data, the more accurate the results of the transport simulation. However, the more temperature grid points with data, the more memory is required to store all the data because the data stored at each grid point contains a full continuous energy (CE) data library.

Several other techniques have been proposed to reduce the memory requirements of this method or to determine cross section values at intermediate temperatures. One method is to store data at closer temperature intervals and then interpolate the stored cross section data Trumbull 2006. Other methods apply a finite-difference scheme to stored pointwise data Hart et al. 2016, perform on-the-fly calculations to apply Doppler broadening to cross sections Yesilyurt, Martin, and Brown 2012; Josey 2015; Yuan, Liu, and Wang 2016, and account for target velocities using rejection sampling Viitanen and Leppänen 2013.

Because multiple ways exist to account for temperature-dependent effects, determining the most appropriate method to use can be difficult. Previous comparisons of a piecewise-linear exact integration, a Gauss–Legendre quadrature, and a Gauss–Hermite quadrature to evaluate Doppler-broadened cross sections showed the exact integration method is the slowest of the three with respect to wall clock Romano and Trumbull 2015. This work also showed an increase in the run time by at least an order of magnitude when the Gauss–Hermite quadrature Doppler broadening method was used on the fly compared with when Doppler broadening was not applied. Yuan et al. Yuan, Liu, and Wang 2016 also compared these methods as implemented in RMC, an MC code developed by Tsinghua University. Their work found that the Gauss–Legendre quadrature method of on-the-fly Doppler broadening was more accurate to the reference case than the Gauss–Hermite quadrature but required more run time. Both of these comparisons focused on on-the-fly Doppler broadening methods and considered only accuracy and run time in evaluating the performance of these methods.

In this paper, the temperature-dependent effects of different physics models used in the Shift MC code Pandya et al. 2016 are demonstrated and characterized. Additionally, the computational performance and trade-offs in memory and run time for each of the methods are quantified. Four methods are compared: the traditional method of storing cross section data at a select few temperatures (the *Library method*), calculating all the interpolated cross sections in a 1D and a 2D space before radiation transport is simulated (the *1D Preprocess* and *2D Preprocess methods*) Hart et al. 2016, and an on-the-fly method using a WMP technique (the *WMP method*) Josey et al. 2016. These methods were used in three radiation transport problems, and the results were compared with respect to accuracy, run time, and memory usage. Previous work Romano and Trumbull 2015; Yuan, Liu, and Wang 2016 compared the accuracy of Doppler broadening methods based on the resulting cross section values, not the results of their application to transport problems. This work is intended to characterize the performance of each of these methods and inform users on the most appropriate method to use in an MC simulation. The advantages and disadvantages of each method as implemented in Shift are also identified.

Section 2 provides background information on the methods and calculations of each Doppler broadening method investigated in this work. Section 3 provides an overview of how the methods were compared and briefly describes each problem used (a 1D spherical shell geometry and two pressurized water reactor (PWR) assembly geometries. Section 4 describes the geometry and results from the 1D spherical shell problem. Section 5 describes the geometries and results from the 2D and 3D PWR assembly problems. Finally, Section 6 provides concluding remarks.

2. DOPPLER BROADENING METHODS

The following sections provide an overview of the mathematics used by each Doppler broadening method investigated in this work—Library, Preprocess, and WMP—over each primary energy range: thermal, resolved resonance region (RRR), unresolved resonance region (URR), and fast. The sections also explain how each method is implemented in Shift to processes 1D (energy dependence only) and 2D (energy and exit angle dependence) cross section data for chemically bound and unbound states.

2.1 LIBRARY METHOD

The first Doppler broadening method is the Library method, the traditional method of temperature-dependent cross section evaluation. Pointwise cross section data at 0 K are stored in the Evaluated Nuclear Data File (ENDF) library Brown and al. 2018, which is then processed through codes such as AMPX Dunn and Greene, n.d. or NJOY Macfarlane 2000. These codes apply the SIGMA1 kernel broadening method Cullen and Weisbin 1976 to tabulated cross section data to produce temperature-dependent pointwise cross sections. These tabulated cross sections can then be linearly interpolated, which allowed for the development of the method proposed by Trumbull Trumbull 2006. However, using this method requires a fine temperature grid (less than $\Delta_T = 28$ K for some nuclides) to achieve accuracy within 0.1% of the value from NJOY. This method of Doppler broadening cross section data also requires a unified energy grid on which to interpolate the cross section data, which is not always available.

Therefore, to reduce memory requirements, cross section data are stored at only a select few temperatures in Shift. Temperatures with cross section data vary by nuclide. If a temperature without cross section data is used in a problem, then data at the closest temperature with cross section data are used. This process is used for 1D cross sections in thermal, RRR, and fast energies for both chemically bound and unbound systems. In the URR, cross section values at the closest available temperature are pulled from the probability tables of AMPX. When the Library method is used for 2D cross section data, data at the closest available temperature are used from the AMPX library for any system in the RRR, URR, and fast energy ranges. In the thermal energy range, unbound systems sample from the Maxwellian distribution of energies for gaseous particles, and bound systems use values of the $S(\alpha,\beta)$ equation at the closest available temperature.

The memory usage of this method is expected to scale linearly with the number of temperatures with cross section data and will be the largest of any method of a fixed accuracy. This method is expected to have quick run times because no additional calculations are performed to determine the cross section values. However, using data at only specific temperatures with no interpolation between the temperatures means that solutions to radiation transport problems may lose accuracy in favor of speed and reduced memory. This loss of accuracy is of great concern when temperatures are much higher or lower than the stored values or in high-fidelity systems in which neutronics are coupled to thermal hydraulic feedback.

2.2 PREPROCESS METHOD

The next method used in this work is the Preprocess method. This method calculates cross section values using data stored in cross section libraries before radiation transport is simulated. The calculated cross sections are then stored in memory throughout the duration of the simulation. The exact mathematics of the method are based on if the cross section is dependent on energy only (1D) or dependent on energy and angle (2D). Therefore, this method is split into two methods: Preprocess 1D and Preprocess 2D.

2.2.1 Preprocess 1D Method

The Preprocess 1D method uses a finite-difference method on the stored 1D cross section data Hart et al. 2016 based on the Leal–Hwang scattering method Leal and Hwang 1987 in which the Doppler broadening cross sections satisfy

$$\frac{\partial^2 \sigma}{\partial E^2} = \frac{\partial \sigma}{\partial T}. \tag{1}$$

An explicit finite-difference formalism is applied using an energy grid (denoted with i) and temperature grid (denoted with j). The finite difference can also be applied in momentum space, using a grid of $\sqrt{E}$ rather than energy Hart et al. 2016. The first and second derivatives are expanded in a Taylor series to calculate the cross section at any energy grid point E_i and temperature T_{j+1}. Applying the finite difference yields Eq. 2,

$$\sigma_i^{j+1} = s\left(\sigma_{i+1}^{j} + a\sigma_i^j + \sigma_{i-1}^j\right), \tag{2}$$

in which σ is the cross section function, i is the energy grid index, j is the temperature grid index, δu is the energy grid mesh size, T is the temperature, $s = \frac{\delta T}{(\delta u)^2}$, and $a = \frac{1-2s}{s}$ Leal and Hwang 1987. The temperature grid mesh size must be small (approximately 1 K) to have sufficient accuracy relative to the reference cross section values at intermediate energy ranges Hart et al. 2016. When the finite-difference formalism is applied to very low and very high energies, the error increases between the reference cross section values and the calculated values. The increased error is caused by inaccuracies or missing data in surrounding data points used in the finite-difference method and can be alleviated by adding additional points beyond the known energy range and extrapolating Hart et al. 2016.

In Shift, the Preprocess 1D method applies this finite-difference scheme (referred to as the Leal–Hwang method in this report) to 1D cross section data for any system in the RRR and fast energy ranges. In the thermal energy range, the Leal–Hwang method is applied to unbound systems, but in bound systems a linear interpolation is applied on the ENDF thermal scattering sublibrary. The distinction between bound and unbound systems improves accuracy relative to the reference cross section values at low energies Hart et al. 2016. In URR energies, the probability tables values are interpolated to calculate a cross section value at the desired temperature. The Preprocess 1D method applies the same calculation methodology as the Library method for 2D cross section data.

The Preprocess 1D method is expected to have improved accuracy over the library method because it calculates cross section data for the specified temperature. The calculations in this method are performed before the transport process is simulated, so this method is expected to have run times similar to those of the library method. However, the calculated values are stored in memory throughout the duration of the problem, meaning that additional memory is used compared with storing just the initial library of cross section data.

2.2.2 Preprocess 2D Method

The Preprocess 2D method uses a unit-based interpolation scheme on the probability distributions of the double-differential cross sections Hart et al. 2016. This method is primarily applied to thermal moderators, in which the crystalline effects on thermal neutrons affect the neutron movement. This method uses the cumulative probability distribution functions and probability distribution functions of the double-differential scattering cross section data stored in the APMX CE library. The method linearly interpolates on the cosine (μ) and energy (E) probabilities (p) based on the incident energy of the neutron (E_{in}). By interpolating on the cosines, the interpolation takes the form shown in Eq. 3 Hart et al. 2016.

$$p(\mu|E_{in},T) = p(\mu|E_{in},T_i) + \frac{T-T_i}{T_{i+1}-T_i}\left[p(\mu|E_{in},T_{i+1}) - p(\mu|E_{in},T_i)\right]. \tag{3}$$

To determine the outgoing energy probabilities, a unit-base normalization is applied before the interpolation. This normalization is needed when the energy range is not constant between temperatures or incoming energies to prevent artificial peaks in the data when the distributions shift as a function of energy Hart et al. 2016.

In the RRR, URR, and fast energy ranges, the linear interpolations are applied to the 2D cross section data stored in AMPX. For unbound systems in the thermal energy range, the Preprocess 2D method samples the Maxwellian distribution describing the speed of the target material. For bound systems in the thermal energy range, the $S(\alpha,\beta)$ equation is linearly interpolated to provide a value at the desired temperature.

Based on its calculations, this method is expected to have improved accuracy for bound systems over the Preprocess 1D method because of the interpolation of the $S(\alpha,\beta)$ scattering data and 2D cross section data. The Preprocess 2D method is expected to have similar memory requirements as the Preprocess 1D method because they both store calculated cross section data throughout the entire transport problem. It is also expected to have similar or longer run times compared with the Preprocess 1D method because of the additional calculations used for the 2D cross section data.

2.3 WINDOWED MULTIPOLE METHOD

The WMP method Josey et al. 2016 performs Doppler broadening on-the-fly (i.e., during an MC simulation) using a temperature-independent WMP data library. This method relies on the rigorous pole representation of the cross section Hwang 1987, referred to in later work as the multipole representation Forget, Xu, and Smith 2014. The multipole representation is based on the observation that the standard R-matrix Wigner and Eisenbud 1947 form of the cross section can be reasonably approximated as a rational function in $\sqrt{E}$ space. A partial fraction expansion can be performed on this rational function using the residue method. This provides an expression for the cross section in terms of poles (p), which are singularities in the complex plane, and residues (r), which are proportional to the path integrals around these singularities. For some incident energy E, the 0 K cross section for reaction x can be expressed as

$$\sigma_x(E, 0\,\mathrm{K}) = \frac{1}{E}\sum_j \Re\left[\frac{-ir_{x,j}}{p_j - \sqrt{E}}\right], \tag{4}$$

where $\Re$ is the real part operator. This expression can be analytically Doppler broadened using the Solbrig kernel Solbrig 1961 to temperature T using Eq. 5,

$$\sigma_x(E,\xi) = \frac{1}{2E\sqrt{\xi}}\sum_j \Re\left[\sqrt{\pi}r_{xj}W\left(\frac{\sqrt{E}-p_j}{2\sqrt{\xi}}\right)\right], \tag{5}$$

where ξ is expressed in terms of the Boltzmann constant (k_B) and atomic mass of the target nucleus (A),

$$\xi = \frac{k_B T}{4A}, \tag{6}$$

and W is the Faddeeva function. Because evaluating the Faddeeva function on the fly is computationally expensive, the summation in Eq. 5 is truncated such that it is only evaluated for the subset of poles that

contribute the most to the cross section. These important poles (i.e., poles for which $[\Re(p)]^2$ is close to the incident energy) are those nearby in $\sqrt{E}$ space. This truncation is accomplished by subdividing energy space into a series of nonoverlapping windows spaced uniformly in $\sqrt{E}$ space. For each window, the range of important poles is stored and denoted by $[w_{\min}, w_{\max})$. The contributions from poles that are far away in $\sqrt{E}$ space (i.e., outside of the $[w_{\min}, w_{\max}]$ range) are smooth and can be effectively approximated by a polynomial fit. Applying this truncation and polynomial fit, the 0 K cross section becomes

$$\sigma_x(E, 0\,\mathrm{K}) = \frac{1}{E} \sum_{j=w_{\min}}^{w_{\max}} \Re\left[\frac{-ir_{x,j}}{p_j - \sqrt{E}}\right] + \sum_{n=0}^{N-1} a_{x,w,n} E^{(n-2)/2}, \tag{7}$$

which can be Doppler broadened to yield the final equation,

$$\sigma_x(E, \xi) = \frac{1}{2E\sqrt{\xi}} \sum_{j=w_{min}}^{w_{max}} \Re\left[\sqrt{\pi} r_{xj} W\left(\frac{\sqrt{E} - p_j}{2\sqrt{\xi}}\right)\right] + \sum_{n=0}^{N-1} a_{w,n,x} \mathfrak{D}_n, \tag{8}$$

with

$$\mathfrak{D}_n = \begin{cases} \frac{1}{E}\mathrm{erf}\left(\frac{\sqrt{E}}{2\sqrt{\xi}}\right) & n = 0, \\ \frac{1}{\sqrt{E}} & n = 1, \\ (2\xi + E)\frac{1}{E}\mathrm{erf}\left(\frac{\sqrt{E}}{2\sqrt{\xi}}\right) + 2\sqrt{\frac{\xi}{\pi E}} e^{-\frac{E}{4\xi}} & n = 2, \\ [2\xi(2n-3) + E]\mathfrak{D}_{n-2} & n = 3, \\ [2\xi(2n-3) + E]\mathfrak{D}_{n-2} - (2\xi)^2(n-2)(n-3)\mathfrak{D}_{n-4} & n \geq 4. \end{cases} \tag{9}$$

A WMP data library consists of poles and reaction-specific residues for each nuclide, as well as $w_{\min}$, $w_{\max}$, and the polynomial coefficients for each window. The WMP library used in this work (adapted from Yu Yu 2022) contains data for 359 nuclides for 5 reactions (total, elastic scatter, absorption, (n, γ), and fission) and is only 56 MB on disk. As a result, this method is expected to have the lowest memory requirements of the methods considered in this work, but a modest increase in run time due to the on-the-fly calculations.

For purposes of this work, the calculations in Eqs. 8 and 9 are referred to as the WMP calculations, while the WMP method refers to the collection of calculations and approximations used across all energy ranges when a user invokes the WMP method in Shift. The WMP calculations are used for 1D cross section data in the RRR energy range and in the thermal energy range for unbound nuclides. As implemented in Shift, the WMP method uses data at the closest library temperature for bound nuclides in the thermal energy range Biondo 2021. In the URR energy range, probability tables at the closest available temperature are used. In the fast energy range, 1D cross section data at the closest available temperature in the cross section library are used, just like in the Library method. For 2D cross section data, the same calculations as the Library method are employed.

2.4 METHOD SUMMARY

Each of these methods employs a different physics method to calculate 1D and 2D cross section values. Table 1 summarizes the calculations employed by each method for 1D cross section data in Shift as a function of energy range and chemical system (bound or unbound). All data required for each method are pulled from the 1D cross section library specified for the radiation transport problem.

Table 1. Summary of the techniques used in each calculation method to evaluate 1D nuclear cross sections. *Closest* means that data stored at the closest temperature are used, *PT* stands for probability tables, *Leal–Hwang* represents the finite-difference method described in Section 2.2.1, and WMP refers to the WMP calculations described in Section 2.3.

		Energy range			
Method	System	Thermal	RRR	URR	Fast
Library	Unbound	Closest	Closest	PT closest	Closest
	Bound	Closest	Closest	PT closest	Closest
Preprocess 1D	Unbound	Leal–Hwang	Leal–Hwang	PT interpolate	Leal–Hwang
	Bound	Interpolate	Leal–Hwang	PT interpolate	Leal–Hwang
Preprocess 2D	Unbound	Leal–Hwang	Leal–Hwang	PT interpolate	Leal–Hwang
	Bound	Interpolate	Leal–Hwang	PT interpolate	Leal–Hwang
WMP	Unbound	WMP	WMP	PT closest	Closest
	Bound	Closest	WMP	PT closest	Closest

Table 2 summarizes the techniques used by each method for 2D cross section data (also called collision data). Data for nonthermal energies are pulled from the 2D cross section library specified for the radiation transport problem.

Table 2. Summary of the techniques used in each calculation method to evaluate collision data.

		Energy range			
Method	System	Thermal	RRR	URR	Fast
Library	Unbound	Maxwell	Closest	Closest	Closest
	Bound	$S(\alpha,\beta)$ closest	Closest	Closest	Closest
Preprocess 1D	Unbound	Maxwell	Closest	Closest	Closest
	Bound	$S(\alpha,\beta)$ closest	Closest	Closest	Closest
Preprocess 2D	Unbound	Maxwell	Interpolate	Interpolate	Interpolate
	Bound	$S(\alpha,\beta)$ interpolate	Interpolate	Interpolate	Interpolate
WMP	Unbound	Maxwell	Closest	Closest	Closest
	Bound	$S(\alpha,\beta)$ closest	Closest	Closest	Closest

3. COMPARISON METHODOLOGY

To compare the results and performance of these four Doppler broadening methods, two radiation transport problems were used: a 1D spherical shell as a fixed source problem and a PWR fuel assembly split into a 2D and 3D geometry as an eigenvalue problem. The spherical shell problem was designed to identify the performance of each method when applied to a geometry with a single nuclide at a single temperature. Thus, the performance characteristics of each method in a simple problem were identified to obtain an in-depth understanding of how the different physics and calculations affect the results of the problem. The PWR assembly was used to apply each method to a geometry with multiple nuclides and multiple temperatures to investigate how small differences in each method's performance in a single nuclide may compound when multiple materials are present. Both problems were used to investigate how each method performs with regard to accuracy, run time, and memory usage. Accuracy of each method was evaluated based on the total flux of the 1D spherical shell geometry and the k_{eff} values of the PWR assembly geometries. The geometry temperatures were varied to provide an additional axis of comparison for the methods.

Each problem was run using Shift and the ENDF/B-VII.1 neutron cross section library. For the Preprocess methods, the temperature tolerance was set at 10^{-5} K, and the delta temperature (which controls the finite-difference mesh size) was set to 0.5 K.

4. ONE-DIMENSIONAL SPHERICAL SHELL PROBLEM

The 1D spherical shell problem was used to compare how each Doppler broadening method performs in a geometry with a single nuclide at a single temperature. The energy-integrated flux, or total flux, of neutrons after traveling through the material was the metric used to compare the accuracy of this problem. Because the total flux was considered, the results do not fully capture the energy dependence of the Doppler broadening methods.

The problem geometry comprised three primary concentric sections surrounded by voids: the source, the shielding material, and the detector, as shown in Fig. 1. A spherical ^{252}Cf neutron source with a radius of 0.1 cm was located at the origin to allow for better repeatability because all radiation transport codes may not support point sources. The energy spectrum of a ^{252}Cf neutron source means most neutrons are born in the fast energy range and then thermalize as they travel through the material. The thermalization of fast neutrons leads to neutrons of all energy ranges in the problem. The void section around the source extended from a radius of 0.1 to 1.3 cm. This part of the geometry was included in the problem for improved repeatability with other transport codes because all codes may not support material adjacent to a source.

The shielding material section was a shell between spheres of radii 1.3 and 25 cm. The shielding material was one of three materials commonly found in nuclear reactors: ^{1}H (in both a bound and unbound system), ^{56}Fe, and ^{90}Zr. Fig. 2 shows the total cross section as a function of energy for each of the nuclides in this problem. The ^{1}H cross section data in Fig. 2 are for an unbound state and do not contain any resonances. However, ^{56}Fe and ^{90}Zr each contain multiple resonances; therefore, the results of using these nuclides are expected to vary greatly depending on the Doppler broadening method used. The number density of each material was calculated to represent three mean free paths in the nuclide shell based on a spectrum-averaged total cross section value at 600 K. A void section surrounded the shielding material section and extended from a radius of 25 to 29.9 cm. The detector region was a shell between spheres of radii 29.9 and 30 cm and was composed of a void material to prevent further attenuation of the neutrons. The neutron flux was tallied in the detector region of the geometry.

This geometry was run multiple times with each shielding material at a uniform temperature ranging from 300 to 900 K in increments of 25 K. These temperatures were selected based on temperatures commonly found in a light-water reactor. Each simulation ran with 100 million particles in analog (i.e., with no variance reduction besides implicit capture). Energy-integrated flux as a function of material temperature was used to compare the accuracy of the methods for the 1D spherical shell geometry. All error bars represent 2σ and are on the order of $10^{-9} \frac{n}{cm^2-s}$.

4.1 BOUND ^{1}H RESULTS

The first nuclide used in the geometry was bound ^{1}H. In the bound system, ^{1}H was bonded to oxygen to form water, and this bond altered how the cross section data was processed (see Table 1). The total flux results for the bound system are shown in Fig. 3.

The flux when using bound ^{1}H increased as a function of temperature as expected for a nuclide without resonances. The Library method showed step changes between different temperatures, signifying the change in which temperature's cross section data were used.

The methods showed generally good agreement, especially at temperatures with stored cross section data. The fluxes from both Preprocess methods were exactly the same as the flux from the Library method at each temperature with cross section data. This agreement was a result of the Leal-Hwang method employed by

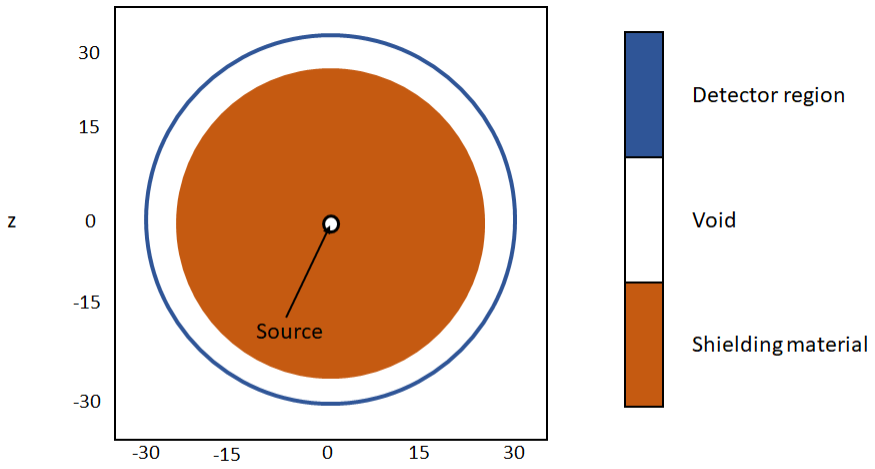

Figure 1. 1D spherical shell problem geometry. The shielding material was varied between bound ^{1}H, unbound ^{1}H, ^{56}Fe, and ^{90}Zr. The shielding material was in an isothermal state, and the temperature was varied between iterations of the geometry.

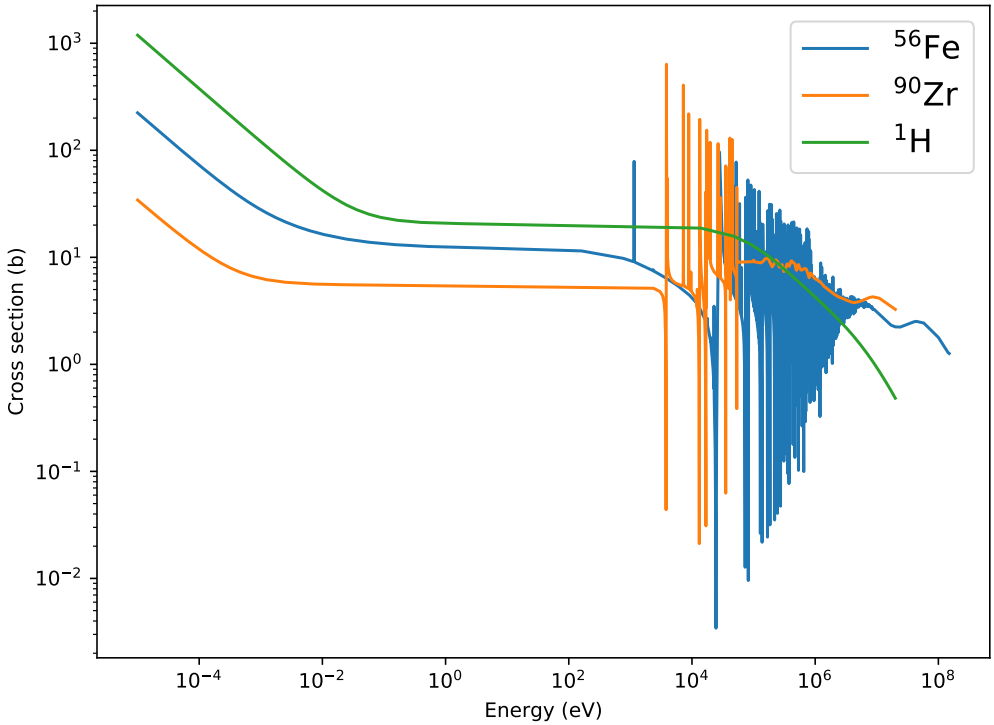

Figure 2. Total cross section of each nuclide used in the 1D spherical shell geometry as a function of energy. These plots were created using data from the Sigma tool from the National Nuclear Data Center BNL,

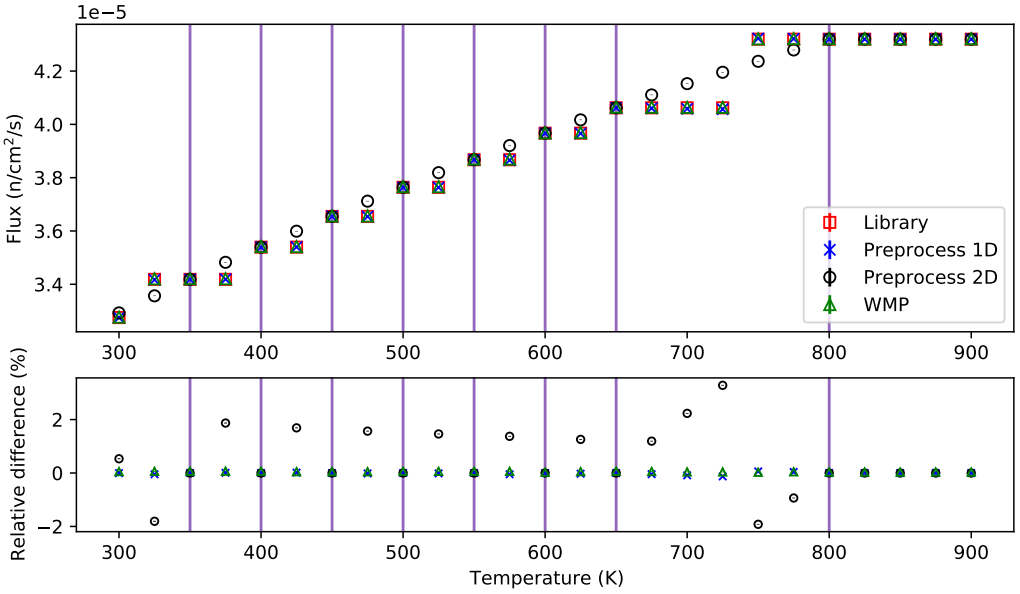

Figure 3. Energy-integrated flux for bound ^{1}H as a function of material temperature. The purple lines show the temperatures at which data were available for the library method. The bottom plot shows the relative difference from the flux from the Library method. The maximum standard deviation of the fluxes was 4.4 $\times$ 10^{-9} n/cm^2/s, and the maximum error in the relative difference was 0.019%.

the Preprocess methods in the RRR and fast energy ranges for bound nuclides. The Leal-Hwang method starts at the stored cross section data; therefore, when a temperature with stored cross section data is used in a problem, no additional calculations take place and the stored value is used. In the thermal and URR energy ranges, the Preprocess methods interpolate on the data, but if the temperature used has cross section data, then again no other calculations are performed and the stored cross section data are used. At temperatures above 800 K, the Preprocess methods also resulted in the same fluxes as the flux obtained using the Library method, despite these temperatures not having cross section data available. This agreement was a result of the lack of cross section data at temperatures above 800 K. Without cross section data at a temperature above the applied temperature, the Leal–Hwang method and the data interpolations were not performed. Therefore, the Preprocess methods used the cross section data at 800 K for each of the temperatures above 800 K.

The WMP method never results in perfect agreement with the Library method, even at temperatures with stored cross section data. The difference in the total fluxes obtained using these two methods was on the order of 10^{-8} $\frac{n}{cm^2}$, which is three orders of magnitude smaller than the total fluxes but more than the standard deviation. The energy spectrum of the two fluxes at 600 K (Fig. 4) shows that the most significant differences in the fluxes were around 0.1 eV and 1 MeV, which are in the thermal and URR energy ranges. These two methods apply the same calculations in these energy ranges, so further investigation is required to determine the cause of these differences.

At temperatures without cross section data below 800 K, the Library method results in a different flux than the other three methods. The differences in flux between the Preprocess 1D and WMP methods and the Library method were on the order of 10^{-8} $\frac{n}{cm^2}$. The difference in flux between the Preprocess 2D method and the Library method was on the order of 10^{-7}, which is two orders of magnitude larger than the standard deviation of the fluxes. The larger difference in the Preprocess 2D method was a result of the calculations for collision data (Table 2) because the Preprocess methods use the same methods to calculate the cross section data. The Preprocess 2D method performs interpolation of the collision data in each of the energy ranges (using S(α,β)

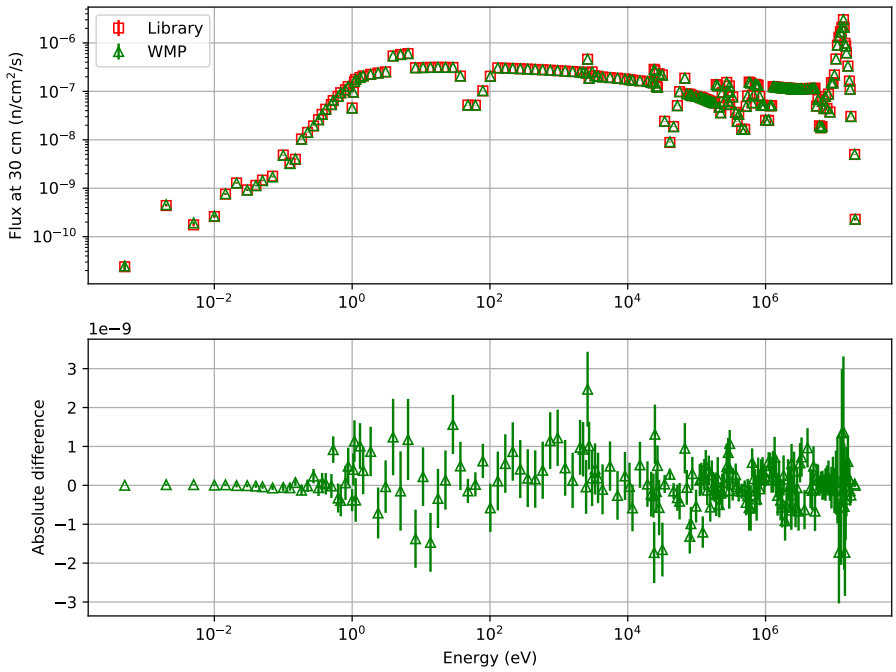

Figure 4. Flux energy spectrum resulting from the library and WMP methods for unbound ^{1}H at 600 K. The bottom plot shows the absolute difference between these two methods. The maximum standard deviation of the fluxes was 1.4 $\times$ 10^{-9}, and the maximum error of the differences was 1.9 $\times$ 10^{-9}.

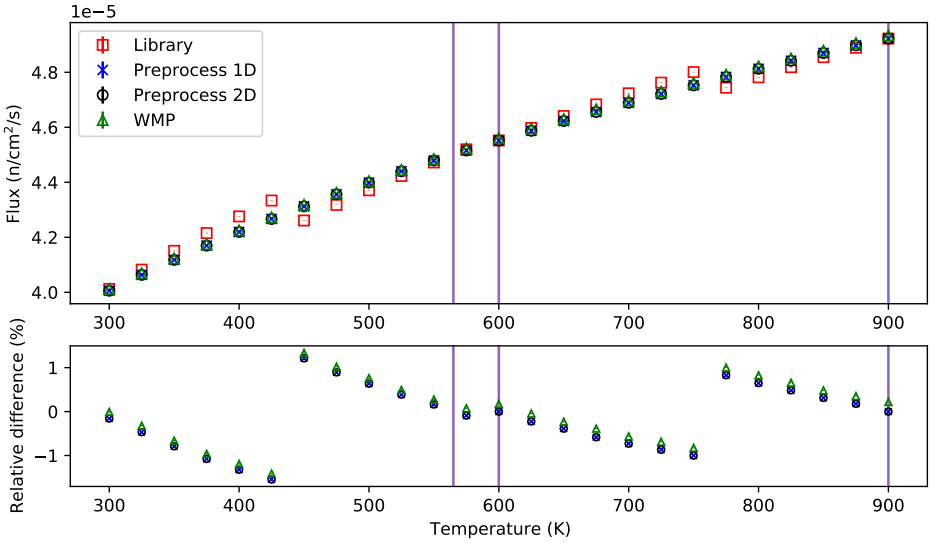

Figure 5. Energy-integrated flux for free ^{1}H as a function of material temperature. The purple lines show the temperatures at which data were available for the Library method. The bottom plot shows the relative difference from the flux from the Library method. The maximum standard deviation in the fluxes was 4.3 $\times$ 10^{-9}, and the maximum error in the relative difference was 0.015%.

data in the thermal energy range for bound system), whereas the other three methods use data at the closest available temperature. The more continuous nature of the flux from the Preprocess 2D method suggests that the interpolation of the collision data results in a more accurate total flux from this method compared with the other methods.

4.2 UNBOUND ^{1}H RESULTS

Fig. 5 shows the total flux for unbound ^{1}H as a function of temperature when each method was used. The fluxes increased as a function of temperature, similar to the trend in the fluxes from using bound ^{1}H. The Library method also exhibited some step changes in these results, although they were smaller in magnitude than the step changes in the flux when using bound ^{1}H. These smaller changes were a result of the difference in treatment of the collision data for bound and unbound systems by the Library method. Most of the flux in these problems was in the thermal energy range (similar to what is shown in Fig. 4), and therefore the treatment of collision data in the thermal energy range has the greatest effect on the results. For bound systems, the Library method uses the S(α,β) data at the closest available temperature but samples the Maxwell distribution of energies for unbound systems. This difference in collision data treatment resulted in the difference in trend of the flux from the Library method in these two systems.

The Preprocess methods resulted in the same flux at every temperature used in this work. This agreement, similar to their disagreement in the bound ^{1}H system, was a result of how these methods treat collision data. In the RRR, URR, and fast energy ranges, the Preprocess 2D method interpolates the collision data and the Preprocess 1D method uses collision data at the closest temperature with data. However, both methods sample the Maxwell distribution of energies in the thermal energy range. The flux in this system was primarily in the thermal energy range, so the similar treatment of the collision data in the thermal energy range dominated the differences in the collision data in the other energy ranges. Additionally, because the nuclide is in an unbound system for this problem, the collision data affects the results much less than for a bound system.

Fluxes for both the WMP and Preprocess methods differed from the flux from the Library method on the order

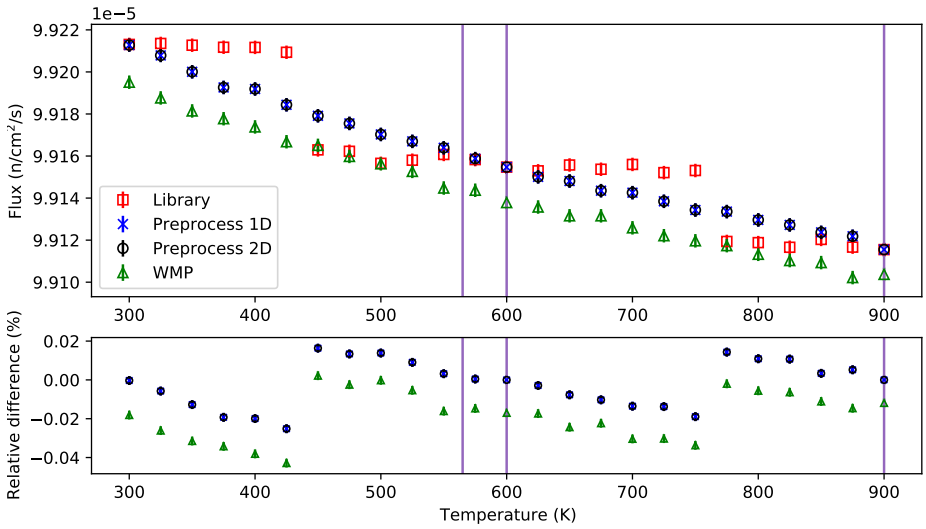

Figure 6. Energy-integrated flux for ^{56}Fe as a function of material temperature. The purple lines show the temperatures at which data were available for the library method. The bottom plot shows the relative difference from the flux from the Library method. The maximum standard deviation of the fluxes was 1.6×10^{-9}, and the maximum error in the relative differences was 0.023%.

of 10^{-7} and differed from one another on the order of 10^{-8}. Similar to the bound ^{1}H system, the difference between the fluxes was primarily in the thermal energy range.

4.3 ^{56}FE RESULTS

The flux through ^{56}Fe using each method, shown in Fig. 6, decreased as a function of temperature because unlike ^{1}H, ^{56}Fe has resonances that broaden with increasing temperature and increase neutron capture. The Library method resulted in step changes when cross section data at a new temperature were used. The WMP and Preprocess methods resulted in more continuous functions.

The WMP method resulted in a smaller flux than the other three methods at each temperature. The differences in the flux from the WMP and those of the other methods were on the order of 10^{-8} n/cm^2/s, which is three orders of magnitude smaller than the values of the flux but one order of magnitude greater than the standard deviation. As Fig. 7 shows, the highest flux is around 0.01–1 MeV in the RRR for ^{56}Fe. In the RRR region, the WMP method employs the multipole calculations, while the Library method uses the data at the closest available temperature and the Preprocess methods apply the Leal-Hwang method, which explains the difference in results

The Preprocess methods resulted in the same flux at every temperature, similar to their agreement in the unbound ^{1}H system. This agreement was observed despite the difference in treatment of collision data because of the diminished effect of collision data treatment for unbound systems. However, the 2D data processing of the 2D Preprocess method is primarily performed for nuclides and materials that are thermal moderators Hart et al. 2016. Therefore, because ^{56}Fe is not a thermal moderator, no additional calculations were performed on the 2D data for this nuclide, resulting in the Preprocess methods yielding the same result.

4.4 ^{90}ZR RESULTS

The flux through ^{90}Zr as a function of temperature when using each method is shown in Fig. 8. The trends of the results were similar to those from ^{56}Fe. The fluxes generally decreased as a function of temperature, the

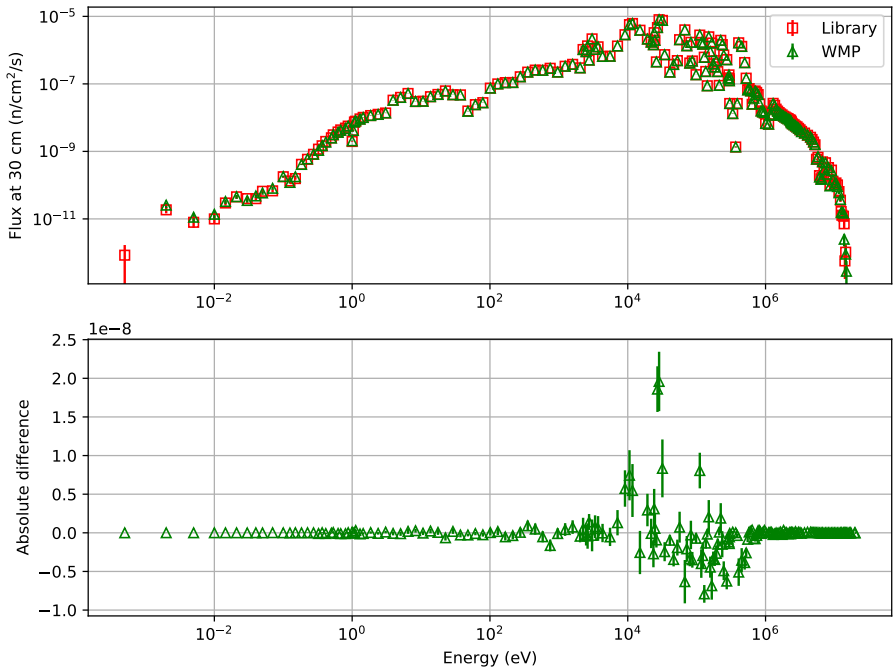

Figure 7. Flux through ^{56}Fe as a function of energy using the Library and WMP methods at 600 K. The bottom plot shows the absolute difference between the two fluxes. The maximum standard deviation of the flux was 2.7 $\times$ 10^{-9}, and the maximum error of the difference was 3.8 $\times$ 10^{-9}.

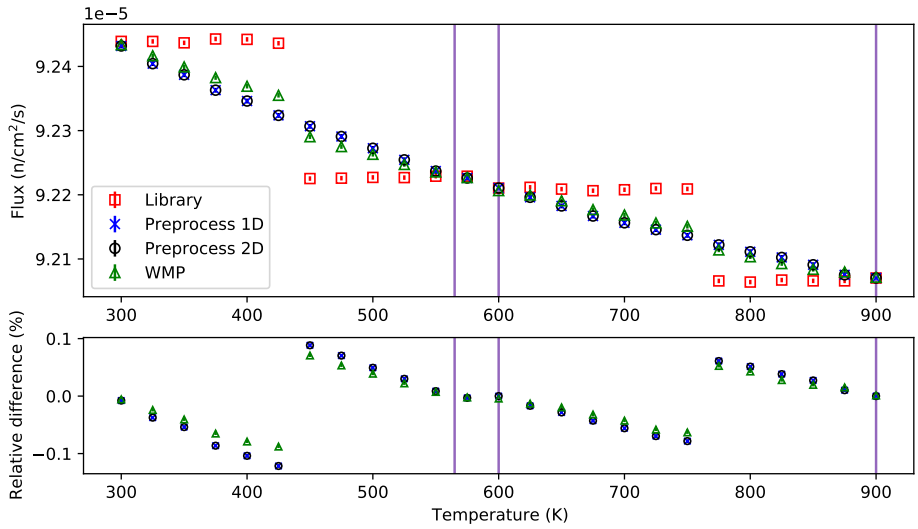

Figure 8. Energy-integrated flux for ^{90}Zr as a function of material temperature. The purple lines show the temperatures at which data were available for the Library method. The bottom plot shows the relative difference from the flux from the Library method. The maximum standard deviation of the fluxes was 1.7×10^{-9}, and the maximum error in the relative differences was 0.027%.

Library method flux showed step changes between temperatures with cross section data, and the other three methods resulted in more continuous functions. The variation between adjacent temperatures in these results appears to be less than the variation between adjacent temperatures in the flux through ^{56}Fe. However, the differences between adjacent temperatures in these results were actually larger, and the total scale of Fig. 8 is larger than that of Fig. 6. Therefore, small differences are magnified in the results of ^{56}Fe but obfuscated somewhat in these results.

Similar to the fluxes through unbound ^{1}H and ^{56}Fe, the Preprocess methods resulted in the same flux at each temperature. The WMP method did not show perfect agreement with the results of the other methods. Qualitatively, the fluxes from the Preprocess methods are continuous with respect to temperature because they interpolate cross sections in both the RRR and URR. The fluxes from the Library method are discontinuous because no interpolation is performed, and fluxes the WMP method has only small discontinuities between because it has a continuous temperature treatment only in the thermal energy range and the RRR. This result is consistent with the variable treatments described in Table 1. The difference in the fluxes from the WMP and Preprocess methods ranged between 7×10^{-10} and 1×10^{-8}, which is larger than the ranges of difference in flux in the other nuclides. The larger range in variation in the fluxes was primarily a result of the different data treatments in the URR .

4.5 PERFORMANCE RESULTS

In addition to understanding the effects of the Doppler broadening methods on the results, it is important to understand their effects on simulation performance. This work focused on the memory required to store the data during the simulation and the time to run the transport simulation.

Figure 9 shows the average memory over the number of processors required for the leakage shell geometry when each nuclide was used. When bound ^{1}H was used, the Preprocess 2D method required significantly more memory than the other methods. The memory required by the Preprocess 2D method was also temperature dependent; generally memory requirements decreased as temperature increased because the collision data

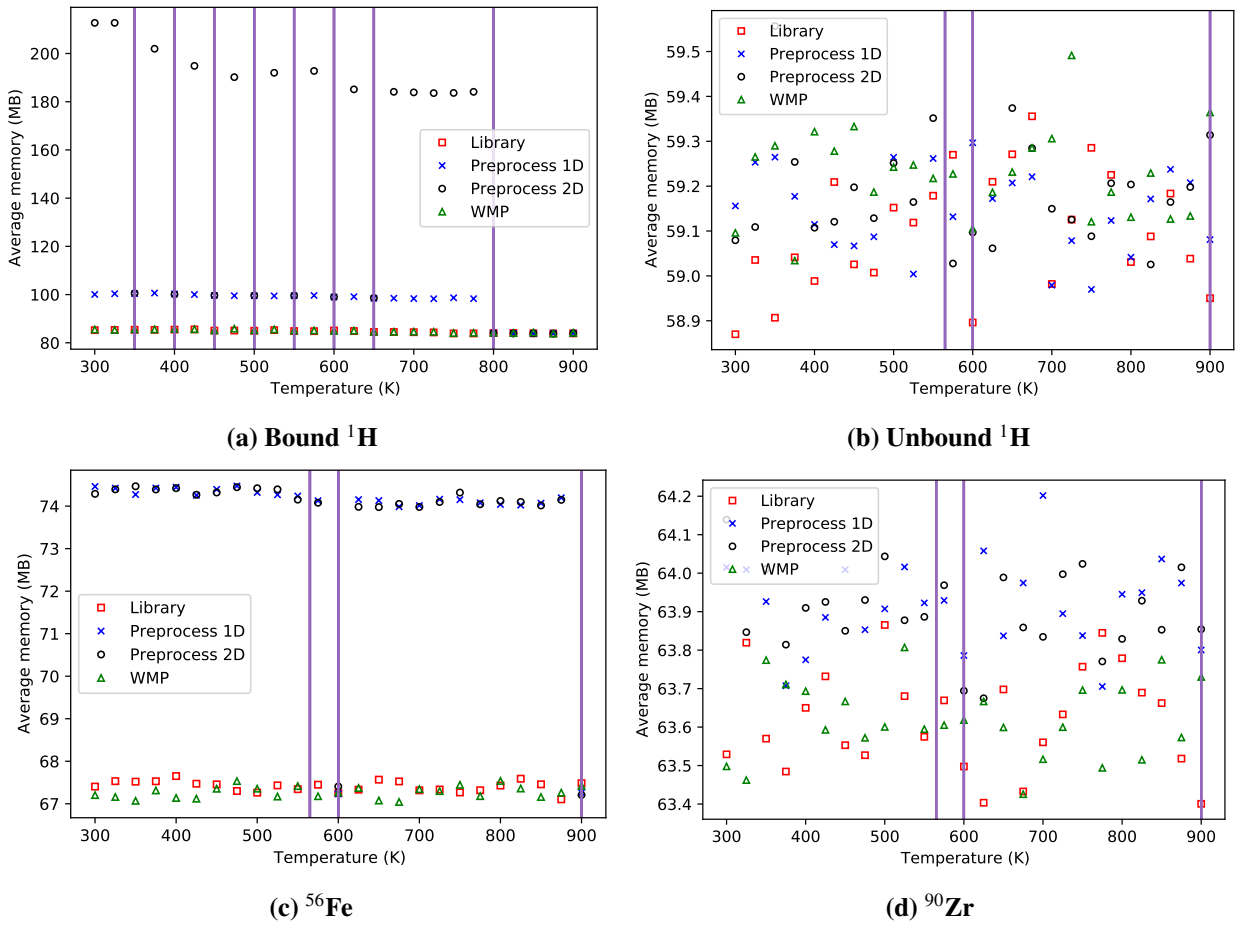

(a) Bound ^{1}H **(b) Unbound ^{1}H**

(c) ^{56}Fe **(d) ^{90}Zr**

Figure 9. Average memory (MB) required per core by each method at every temperature in the 1D spherical shell geometry. The purple lines show the temperatures with cross section data available.

decreases in size as temperature increases. The Preprocess 1D method required the next largest amount of memory. The Preprocess 1D method required more memory than the Library method at temperatures with cross section data despite the methods yielding the same flux. This higher memory usage results from additional temporary data necessary for preprocessing.

The Preprocess methods required the most memory because the interpolated values were stored throughout the simulation. At temperatures with discrete data, the two Preprocess methods had similar memory requirements (within 0.3 MB of each other). At temperatures 800 K and above, all four methods required similar amounts of memory (within 0.5 MB of one another). This result occurred because of the lack of cross section data stored at temperatures above 800 K for bound ^{1}H, meaning that the forward difference calculations of the Preprocess methods were not performed and calculated values were not stored. The WMP and Library methods had similar memory requirements for this system because neither method stores addtional data during a simulation.

The memory required for this problem when using ^{56}Fe showed similar patterns to when bound ^{1}H was used. The Preprocess methods required the most memory, and the WMP method required the least. However, the Preprocess methods required similar amounts of memory at each temperature when using ^{56}Fe compared with the large differences between these two methods when using bound ^{1}H. The Preprocess methods had similar memory requirements in the ^{56}Fe system because in an unbound system both methods store just

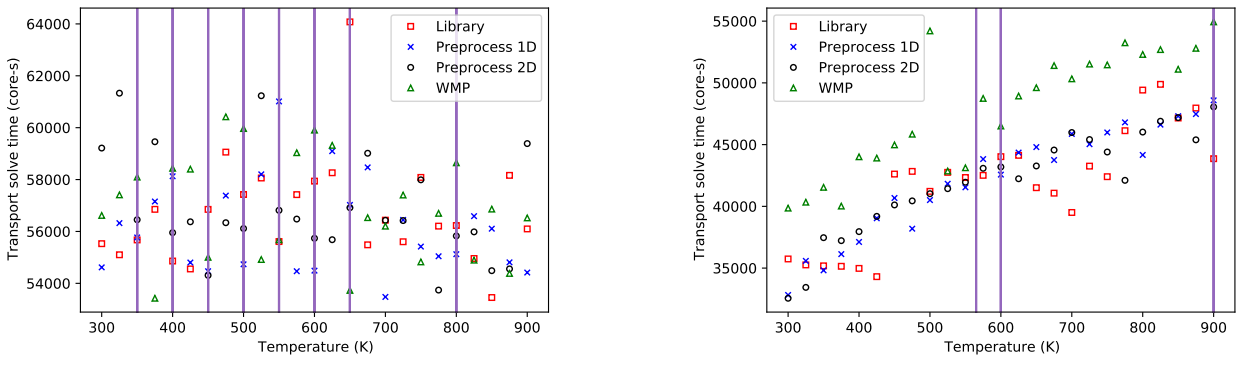

(a) Bound ^{1}H **(b) Unbound ^{1}H**

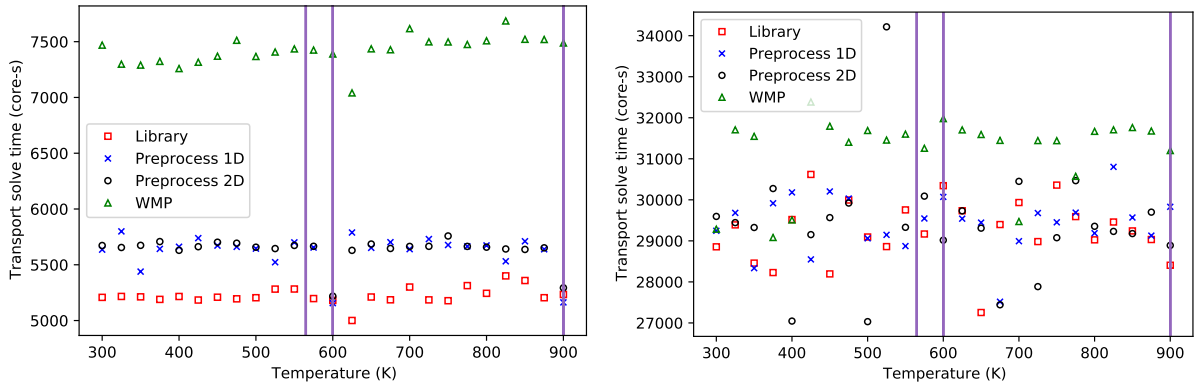

(c) ^{56}Fe **(d) ^{90}Zr**

Figure 10. Time (in core·seconds) required by each method to solve the transport problem at every temperature in the 1D spherical shell geometry. The purple lines show the temperatures with cross section data available.

the cross section data. Whereas in a bound system the 1D method stores the cross section data and the 2D method stores the cross section and collision data. When unbound ^{1}H or ^{90}Zr were used in the geometry, the four methods required similar amounts of memory. The difference in memory requirements and the differences among the methods when using the unbound nuclides resulted from the difference in the number of resonances present in the cross section data of each nuclide. The more resonances a nuclide has, the more memory is required and the larger the differences are among the methods.

Figure 10 shows the amounts of time required to perform the transport simulations using each of the nuclides. When bound ^{1}H was used, no strong trend was observed among the methods, but when the other three nuclides were used, the same trend was observed: the WMP method usually required the most time to complete a transport calculation. This result stems from the WMP method performing the Doppler broadening calculations on-the-fly during the transport solve of the simulation. This trend was not observed when using bound ^{1}H because the WMP method implemented in Shift uses data at the closest available temperature in the thermal energy range (Table 1). Therefore, the WMP method requires a similar amount of time to complete the transport calculation when using a bound nuclide with larger thermal cross sections. For the three unbound nuclides, the two Preprocess methods required similar amounts of time to complete the transport simulation, which does not suggest one Preprocess method is preferable over the other considering these methods resulted in the same flux.

5. PRESSURIZE WATER REACTOR ASSEMBLY PROBLEM

The PWR fuel assembly problem was used to investigate how each method performs in solving a k_{eff} eigenvalue problem in a complex geometry and how the small differences in the results from one nuclide may compound when multiple nuclides are present. The fuel assembly geometry modeled a Westinghouse 17×17 PWR fuel assembly with 3.2% enrichment and was used in a 2D and 3D configuration. Materials present in this geometry included UO_2, H_2O, and Zr cladding, among others.

The 2D assembly geometry (Fig. 11) was based on VERA Problem 2a Godfrey 2014 and contained the radial slice of the assembly at zero power isothermal conditions with reflective boundaries in the x-, y-, and z-directions. The temperature of the assembly was varied to provide a comparison of each method within a complex geometry. Temperatures ranged from 300 to 900 K, in increments of 25 K, and included 293 K and 565 K to provide additional temperatures with cross section data.

The 3D assembly geometry was modeled after VERA problem 6 Godfrey 2014. Figure 11 shows a radial view of this geometry. This geometry was at hot full power with no depletion and included axial and radial temperature variations. Because of the temperature variations within this model, temperature variations were not included as a model variable. The only parameter varied in this geometry was the Doppler broadening calculation method. Hydrogen was assumed to be in a bound state for both the 2D and 3D geometries.

For each problem, 5 inactive cycles and 100 active cycles were completed, with 1 million histories per cycle. The results of these geometries were the k_{eff} value, the transport solve time, nuclide data load time, and the memory used.

5.1 2D ASSEMBLY RESULTS

Fig. 12 shows the k_{eff} as a function of temperature when each Doppler broadening method was used. For all of the nuclides present in the geometry except bound ^{1}, cross section data were available at 293, 565, 600, and 900 K. The k_{eff} generally decreased as a function of temperature because of the additional neutron captures that occurred in the RRR and URR from Doppler broadening. The Library method resulted in large step changes, whereas the other methods resulted in more linear changes in the k_{eff} as a function of temperature.

The step changes when using the Library method resulted from changing the cross section data used from one set of temperatures to another. The more linear behavior of the other three methods resulted from the calculations and interpolation of the available cross section data. The trends in the problem results were consistent with the trends from the flux through ^{56}Fe and ^{90}Zr in the 1D spherical shell. The results from the Preprocess methods and WMP method differed from the Library method results by up to 500 pcm, but the more continuous nature of the the Preprocess and WMP methods suggests that they produce more accurate results than the Library method. Therefore, when using temperatures without cross section data in a complex geometry, the Preprocess and WMP methods are recommended for improved accuracy in the simulation results.

At 293, 600, and 900 K, the Preprocess methods resulted in the same k_{eff} as the Library method. These were the only three temperatures at which all nuclides present had cross section data available (bound ^{1}H did not have data stored at 565 K). At these temperatures, the WMP method resulted in k_{eff} that are 10 ± 8.9, 8.6 ± 9.1, and 10 ± 9.7 pcm different from the k_{eff} from the Library method. The standard deviations for the Library k_{eff} values were approximately 6 pcm. Therefore, these differences were within two standard deviations and were not significant. These results suggest that although the results of a system with a single nuclide may be significant, the differences do not necessarily compound to produce even larger differences in a multimaterial system.

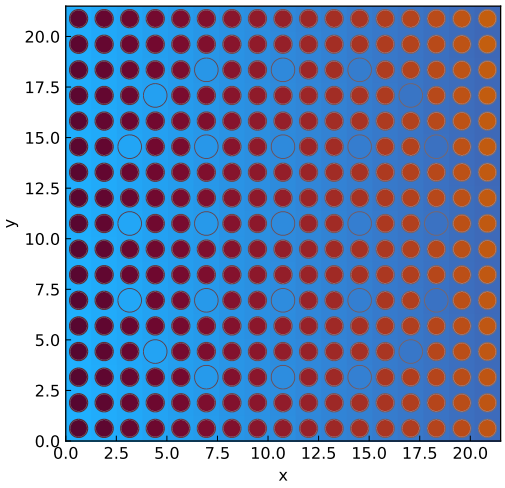

Figure 11. Radial view of the 3D fuel assembly geometry.

Table 3. Difference between the k_{eff} from each Doppler broadening method at 565 K in the 2D PWR assembly and the reference value reported by Godfrey Godfrey 2014.

Method	Difference (pcm)
Library	−72 ± 6.7
Preprocess 1D	−69 ± 6.1
Preprocess 2D	−66 ± 6.5
WMP	−71 ± 7.1

Godfrey reported a reference k_{eff} of 1.182175 ± 1.7 pcm for this geometry at 565 K Godfrey 2014 using the Library method. Table 3 reports the difference between this reference value and the k_{eff} from each method at 565 K. Each Doppler broadening method resulted in a k_{eff} less than the reference value and outside of the propagated error from the reference value. However, Godfrey used an older version of SCALE (SCALE 6.2 compared with SCALE 6.3 in this work) and older cross section data (ENDF 7.0 compared with ENDF 7.1), which likely led to the differences in k_{eff} more than the Doppler broadening method employed.

Tables 4 and 5 report the average and maximum differences in k_{eff}, respectively, from the Doppler broadening methods. The values in these tables support the observations from Fig. 12: the Library method resulted in k_{eff} values that were statistically different than the results of the other methods, whereas the Preprocess and WMP methods produced similar k_{eff} values.

Fig. 13 shows the different performance metrics as a function of temperature for the 2D PWR assembly

Table 4. Average difference in pcm of k_{eff} values between the method listed in each column and the method listed in each row. Blank cells prevent the repeating of values.

	Preprocess 1D	Preprocess 2D	WMP
Library	43 ± 2.0	56 ± 2	43 ± 2.0
Preprocess 1D	—	6.3 ± 1.7	5.7 ± 1.7
Preprocess 2D	—	—	12 ± 2

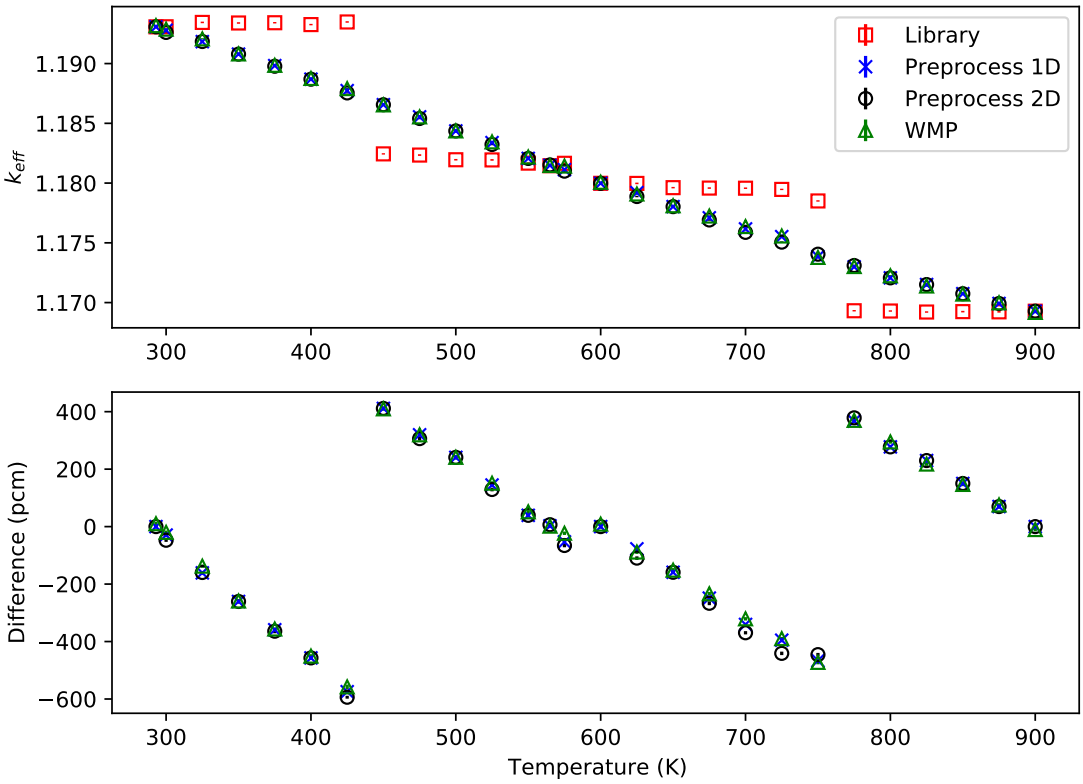

Figure 12. The k_{eff} values using each method for the 2D assembly problem. Bound H was used for each simulation. The difference shown in the bottom plot is relative to the Library method. The maximum standard deviation of the k_{eff} values was 7.8 pcm, and the maximum error in the absolute differences was 7.8 pcm.

Table 5. Maximum difference in pcm of k_{eff} values between the method listed in each column and the method listed in each row. Blank cells in the table prevent the repeating of values.

	Preprocess 1D	Preprocess 2D	WMP
Library	575 ± 9	594 ± 8	558 ± 10
Preprocess 1D	—	46 ± 9	30 ± 9
Preprocess 2D	—	—	51 ± 8

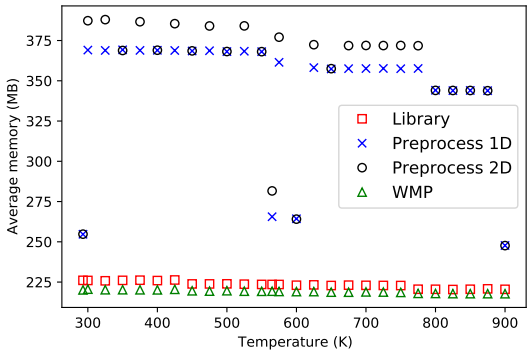

(a) Memory usage as a function of temperature for the 2D assembly problem.

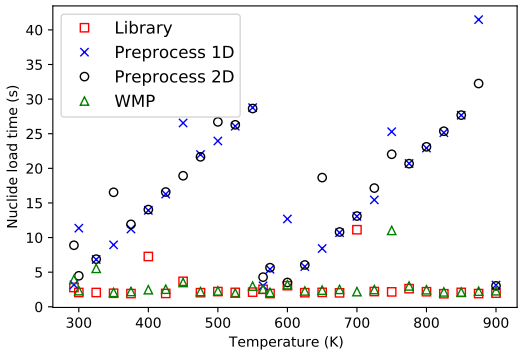

(b) Nuclide data load times as a function of temperature for the 2D assembly problem.

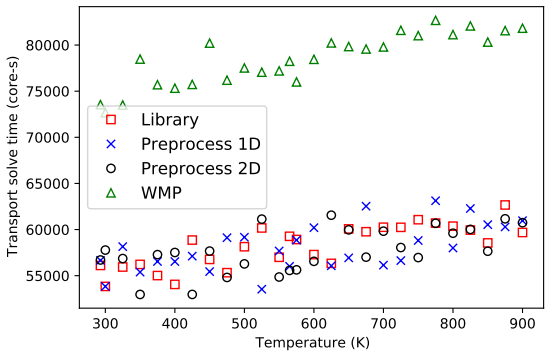

(c) Transport solve times as a function of temperature for the 2D assembly problem.

Figure 13. Performance metrics of the 2D PWR assembly model in an isothermal state using bound hydrogen.

model. These results exhibit some of the trends observed in the results from the 1D spherical shell problem: the Preprocess methods required more memory and time to load the nuclide data than the WMP and Library methods, but the WMP method required more time to run the transport calculation than the other methods. The Preprocess methods requires more time to load the nuclide data because the Leal-Hwang method is applied during this step of a simulation. The transport time increase from using the WMP method was greater than the nuclide data load time increase from using the Preprocess methods, which means that the WMP method increased the total run time more than the Preprocess methods, compared with the Library method.

The memory required for the Preprocess 2D method oscillated because of the multiple temperatures with cross section data available. Most of the nuclides had cross section data available at 293, 565, 600, and 900 K. However, bound ^{1}H had cross section data available at 293, 350, 450, 550, 650, and 800 K. Therefore, the multiple oscillations resulted from the additional temperatures at which bound ^{1}H had cross section data available. These oscillations highlight the effect that the hydrogen had on the results for the 2D assembly model because of its abundance in the geometry.

This problem highlights some of the trade-offs in each Doppler broadening method. The Library method requires minimal memory and time to run, but its results may be less accurate. The Preprocess methods provide more accurate results but at the expense of greater memory requirements. The WMP method also

Table 6. The k_{eff} values and statistical errors for the 3D assembly problem using each Doppler broadening method.

Method	k_{eff}
Library	1.16404 ± 0.00004
Preprocess 1D	1.16237 ± 0.00003
Preprocess 2D	1.16211 ± 0.00003
WMP	1.16188 ± 0.00003

Table 7. Difference in pcm of k_{eff} and propagated error between the method listed in each column and the method listed in each row for the 3D PWR assembly model. Blank cells in the table prevent the repeating of values.

	Preprocess 1D	Preprocess 2D	WMP
Library	167 ± 5	193 ± 5	217 ± 5
Preprocess 1D	—	26 ± 5	50 ± 5
Preprocess 2D	—	—	23 ± 5

provides more accurate results but at the expense of extended run times for the simulation.

5.2 3D ASSEMBLY RESULTS

The 3D fuel assembly geometry provided a comparison among the Doppler broadening methods in a complex geometry with multiple nuclides and multiple temperatures. Table 6 reports the k_{eff} values and their standard deviations for this problem. Table 7 reports the difference in pcm between the k_{eff} values with propagated error. The Library method resulted in the k_{eff} with the largest difference compared with the other values. The Preprocess 2D and WMP methods resulted in the most similar k_{eff} values. Godfrey did not provide a reference solution to this geometry Godfrey 2014, but Kelly et al. provided a reference solution of 1.16424 ± 2.6 pcm on a quarter-core model of the geometry Kelly et al. 2017. With a difference of only 20 ± 5 pcm, the k_{eff} from the Library method was the closest to this reference value. Kelly et al. used a discrete temperature grid between 500–900 K with grid points 50 K apart. Therefore, they employed a method most similar to the Library method in this work, which is consistent with the better agreement between their value and the value from using the Library method.

These k_{eff} values and the differences between them suggest that when multiple materials are used, temperature variations in a problem lead to significant differences in the simulation results produced by different Doppler broadening methods.

Table 8 contains the memory usage and run time data for the 3D fuel assembly problem. These results are consistent with the results of the 2D assembly problem: the WMP method required the least memory but the most time to run the transport simulation and the Preprocess methods required the most memory and the most time to load nuclide data. However, the WMP method took more than twice as long to load the nuclide data than the Library model, whereas in the 2D model, these methods took almost the same time to load the nuclide data. However, the additional time for the WMP method to load the data was still less than the time required by the Preprocess methods and did not greatly affect the total run time of the problem. Additionally, the Library method required the least amount of time to run this problem, whereas it took a comparable amount of time to the Preprocess methods for the 2D assembly model. This result suggests that in more complex geometries, the Library method performs well with regard to memory and transport solve time.

Table 8. Memory usage (per core), load time (per core), and run time (integrated over cores) results for each method in the 3D PWR assembly problem.

Method	Average memory (MB)	Load time (s)	Transport time (core·s)
Library	446	6	4.8×10^5
Preprocess 1D	1135	31	5.2×10^5
Preprocess 2D	1230	34	5.5×10^5
WMP	431	16	6.1×10^5

6. CONCLUSIONS

This work compared the results from using different methods to calculate Doppler broadened cross section values in Shift. The Library, Preprocess 1D, Preprocess 2D, and WMP methods were compared based on the results of radiation transport problems, memory usage, nuclide load time, and transport solve time.

Through examination of each method's performance in a geometry with a single nuclide at a single temperature (the 1D spherical shell problem), this work identified how the treatment of cross section and collision data affects the neutron flux through different materials. The treatment of collision data does not have an effect on the flux through unbound nuclides, but it does have a large effect on the flux through bound nuclides. Small, expected differences in the flux were observed between each of the methods, with the WMP and Preprocess methods resulting in the smallest differences. The performance metrics (transport solve time and memory) of these methods became more distinguishable as the number of resonances of the nuclide used increased.

Next, the performance of the methods in PWR assembly models was compared. In a 2D model, their performance in a multimaterial system at a single temperature was compared. The results for this model were consistent with those for the single nuclide model, but the effect of the methods on the performance metrics was much more pronounced in the 2D PWR model. Then, in a 3D PWR model, the material temperatures were varied (i.e., the material was no longer in an isothermal state) to compare the effect of changing temperatures on the results. The introduction of multiple temperatures caused greater variations in the k_{eff} values of the 3D PWR model.

In each of the problems, trade-offs of each Doppler broadening method were identified. The Library method requires minimal memory and run time but may produce less accurate results. The Preprocess methods provide more accurate results but at the expense of greater memory requirements. The WMP method also provides more accurate results but at the expense of longer simulation run times. Therefore, users are advised to select their Doppler broadening method based on which two of the three method characteristics—accuracy, memory, and simulation run time—are most important.

6.1 FUTURE WORK

This work provides a foundation for characterizing and comparing the performance of different Doppler broadening methods in an MC code. This work can be expanded through further investigations. A suggestion for future work is to further compare these methods, including comparing the accuracy of the results obtained through these methods in Shift and results obtained through transport in other MC codes, such as OpenMC Romano and Forget 2013. It would also be valuable to compare these methods when applied to more standardized problems, such as the Benchmarks for Evaluation and Validation of Reactor Simulations (BEAVRS) model Horelik et al. 2013, using the same metrics used in this work.

Lastly, comparison of the performance of these Doppler broadening methods on a GPU system would also be valuable because many GPU systems and the Shift implementation for GPUs are memory bound. Therefore, understanding how each Doppler broadening method performs on these systems can inform users on whether the method will affect how their simulations run.

ACKNOWLEDGEMENTS

This work was completed in part through the Nuclear Engineering Science Laboratory Synthesis program at Oak Ridge National Laboratory.

This material is based upon work supported under a University Nuclear Leadership Program Graduate Fellowship.

This research was supported by the Exascale Computing Project (ECP), project number 17-SC-20-SC. The ECP is a collaborative effort of two DOE organizations, the Office of Science and the National Nuclear Security Administration, that are responsible for the planning and preparation of a capable exascale ecosystem—including software, applications, hardware, advanced system engineering, and early testbed platforms—to support the nation's exascale computing imperative.

The authors thank Tara Pandya and Cihangir Celik for their helpful reviews and the Exnihilo team for their assistance.

7. REFERENCES

Biondo, Elliott. 2021. *Implementation of the Windowed Multipole Method in Shift* [in English]. Technical report ORNL/TM-2021/2056. Oak Ridge National Lab. (ORNL), Oak Ridge, TN (United States), August. Accessed November 19, 2021. https://doi.org/10.2172/1818696. https://www.osti.gov/biblio/1818696-implementation-windowed-multipole-method-shift.

BNL. *Sigma Plots.* Accessed November 8, 2021. https://www.nndc.bnl.gov/sigma/getPlot.jsp?evalid=14960&mf=3&mt=1&nsub=10.

Brown, D. A., and et al. 2018. "ENDF/B-VIII.0: The 8th Major Release of the Nuclear Reaction Data Library with CIELO-project Cross Sections, New Standards and Thermal Scattering Data" [in en]. Publisher: Academic Press, *Nuclear Data Sheets* 148 (February): 1–142. ISSN: 0090-3752, accessed May 20, 2021. https://doi.org/10.1016/j.nds.2018.02.001. http://www.sciencedirect.com/science/article/pii/S0090375218300206.

Cullen, Dermott E., and Charles R. Weisbin. 1976. "Exact Doppler Broadening of Tabulated Cross Sections." Publisher: Taylor & Francis, *Nuclear Science and Engineering* 60, no. 3 (July): 199–229. ISSN: 0029-5639, accessed October 25, 2021. https://doi.org/10.13182/NSE76-1.

Dunn, M E, and N M Greene. n.d. "AMPX-2000: A Cross-Section Processing System for Generating Nuclear Data for Criticality Safety Applications" [in en], 5.

Forget, Benoit, Sheng Xu, and Kord Smith. 2014. "Direct Doppler broadening in Monte Carlo simulations using the multipole representation" [in en]. *Annals of Nuclear Energy* 64 (February): 78–85. ISSN: 0306-4549, accessed March 10, 2020. https://doi.org/10.1016/j.anucene.2013.09.043. http://www.sciencedirect.com/science/article/pii/S0306454913005136.

Godfrey, Andrew T. 2014. *VERA Core Physics Benchmark Progression Problem Specifications* [in en]. Technical report CASL-U-2012-0131-004. Oak Ridge National Lab., August.

Hart, Shane W.D., Cihangir Celik, G. Ivan Maldonado, and Luiz Leal. 2016. "Creation of problem-dependent Doppler-broadened cross sections in the KENO Monte Carlo code" [in en]. *Annals of Nuclear Energy* 88 (February): 49–56. ISSN: 03064549, accessed April 8, 2020. https://doi.org/10.1016/j.anucene.2015.10.011. https://linkinghub.elsevier.com/retrieve/pii/S0306454915004909.

Horelik, Nicholas, Bryan Herman, Benoit Forget, and Kord Smith. 2013. "Benchmark for evaluation and validation of reactor simulations (BEAVRS), v1. 0.1." In *Proc. Int. Conf. Mathematics and Computational Methods Applied to Nuc. Sci. & Eng,* 5–9.

Hwang, R. N. 1987. "A Rigorous Pole Representation of Multilevel Cross Sections and Its Practical Applications." Publisher: Taylor & Francis, *Nuclear Science and Engineering* 96, no. 3 (July): 192–209. ISSN: 0029-5639, accessed May 24, 2021. https://doi.org/10.13182/NSE87-A16381.

Josey, C., P. Ducru, B. Forget, and K. Smith. 2016. "Windowed multipole for cross section Doppler broadening" [in en]. *Journal of Computational Physics* 307 (February): 715–727. ISSN: 0021-9991, accessed March 10, 2020. https://doi.org/10.1016/j.jcp.2015.08.013. http://www.sciencedirect.com/science/article/pii/S002199911500532X.

Josey, Colin. 2015. “Windowed multipole : an efficient Doppler broadening technique for Monte Carlo” [in eng]. Accepted: 2016-07-18T20:03:10Z Journal Abbreviation: Efficient Doppler broadening technique for Monte Carlo. Thesis, Massachusetts Institute of Technology. Accessed March 10, 2020. https://dspace.mit.edu/handle/1721.1/103708.

Kelly, Daniel J., Ann E. Kelly, Brian N. Aviles, Andrew T. Godfrey, Robert K. Salko, and Benjamin S. Collins. 2017. “MC21/CTF and VERA multiphysics solutions to VERA core physics benchmark progression problems 6 and 7” [in en]. *Nuclear Engineering and Technology* 49, no. 6 (September): 1326–1338. ISSN: 17385733, accessed May 11, 2023. https://doi.org/10.1016/j.net.2017.07.016. https://linkinghub.elsevier.com/retrieve/pii/S1738573317302978.

Leal, L. C., and R. N. Hwang. 1987. “Finite difference method for treating the Doppler broadening of neutron cross sections” [in en]. *Transactions of the American Nuclear Society* 55 p. 340-342. ISSN: ISSN 0003-018X, accessed March 10, 2020. http://inis.iaea.org/Search/search.aspx?orig_q=RN:20003602.

Macfarlane, Robert E. 2000. *Code System for Producing Pointwise and Multigroup Neutron and Photon Cross Sections from ENDF/B Data.* Technical report. Oak Ridge National Laboratory (ORNL), Oak Ridge, TN (United States).

Pandya, Tara M., Seth R. Johnson, Thomas M. Evans, Gregory G. Davidson, Steven P. Hamilton, and Andrew T. Godfrey. 2016. “Implementation, capabilities, and benchmarking of Shift, a massively parallel Monte Carlo radiation transport code” [in en]. *Journal of Computational Physics* 308 (March): 239–272. ISSN: 0021-9991, accessed May 20, 2021. https://doi.org/10.1016/j.jcp.2015.12.037. https://www.sciencedirect.com/science/article/pii/S0021999115008566.

Romano, Paul K., and Benoit Forget. 2013. “The OpenMC Monte Carlo particle transport code” [in en]. *Annals of Nuclear Energy* 51 (January): 274–281. ISSN: 0306-4549, accessed May 20, 2021. https://doi.org/10.1016/j.anucene.2012.06.040. https://www.sciencedirect.com/science/article/pii/S0306454912003283.

Romano, Paul K., and Timothy H. Trumbull. 2015. “Comparison of algorithms for Doppler broadening pointwise tabulated cross sections” [in en]. *Annals of Nuclear Energy* 75 (January): 358–364. ISSN: 0306-4549, accessed May 20, 2021. https://doi.org/10.1016/j.anucene.2014.08.046. https://www.sciencedirect.com/science/article/pii/S0306454914004460.

Solbrig, A. W. 1961. “Doppler Broadening of Low-Energy Neutron Resonances” [in en]. *Nuclear Science and Engineering* 10, no. 2 (June): 167–168. ISSN: 0029-5639, 1943-748X, accessed May 25, 2021. https://doi.org/10.13182/NSE61-A25954. https://www.tandfonline.com/doi/full/10.13182/NSE61-A25954.

Trumbull, T. H. 2006. “Treatment of Nuclear Data for Transport Problems Containing Detailed Temperature Distributions.” Publisher: Taylor & Francis, *Nuclear Technology* 156, no. 1 (October): 75–86. ISSN: 0029-5450, accessed May 26, 2021. https://doi.org/10.13182/NT156-75.

Viitanen, Tuomas, and Jaakko Leppänen. 2013. “Optimizing the implementation of the target motion sampling temperature treatment technique: How fast can it get?” [In English]. In *Proceedings: International Conference on Mathematics and Computational Methods Applied to Nuclear Science & Engineering, M&C 2013,* 950–961. Accessed March 19, 2020. https://cris.vtt.fi/en/publications/optimizing-the-implementation-of-the-target-motion-sampling-tempe.

Wigner, E. P., and L. Eisenbud. 1947. “Higher Angular Momenta and Long Range Interaction in Resonance Reactions.” *Phys. Rev.* 72 (1): 29–41. https://doi.org/10.1103/PhysRev.72.29. https://link.aps.org/doi/10.1103/PhysRev.72.29.

Yesilyurt, Gokhan, William R. Martin, and Forrest B. Brown. 2012. "On-the-Fly Doppler Broadening for Monte Carlo Codes." Publisher: Taylor & Francis, *Nuclear Science and Engineering* 171, no. 3 (July): 239–257. ISSN: 0029-5639, accessed May 26, 2021. https://doi.org/10.13182/NSE11-67.

Yu, Jiankai. 2022. *wmp-endfbvii.1*. https://github.com/jiankai-yu/wmp-endfbvii.1. Commit: 7887b3144cc579c4a449c2d82ba78

Yuan, Yuan, Schichang Liu, and Kan Wang. 2016. "Implementation and Comparison of Different algorithms for on the Fly Doppler Broadening in RMC Code." In *Transactions of the American Nuclear Soceity Annual Meeting,* vol. 114. New Orleans, LA: American Nuclear Society, June. Accessed September 13, 2022. https://epubs.ans.org/?a=38677&_ga=2.183141478.1909905103.1663006862-287406757.1598467895.